Progress In Electromagnetics Research, PIER 49, 257–271, 2004

PARABOLIC EQUATION SOLUTION OF TROPOSPHERIC WAVE PROPAGATION USING FEM

S. A. Isaakidis and T. D. Xenos

Aristotle University of Thessaloniki
Department of Electrical and Computer Engineering
54006 Thessaloniki, Greece

Abstract—In this work, the parabolic equation applied on radiowave and microwave tropospheric propagation, properly manipulated, and resulting in a one-dimensional form, is solved using the Finite Element Method (FEM). The necessary vertical tropospheric profile characteristics are assigned to each mesh element, while the solution advances in small and constant range segments, each excited by the solution of the previous step. This is leading to a marching algorithm, similar to the widely used Split Step formulation. The surface boundary conditions including the wave polarization and surface conductivity properties are directly applied to the FEM system of equations. Since the FEM system returns the total solution, a technique for the separation of the transmitted and reflected waves is also presented. This method is based on the application of the Discrete Fourier Transform (DFT) in the space domain, which allows for the separation of the existing wave components. Finally, abnormal tropospheric condition propagation is being employed to assess the method, while the results are compared to those obtained using the Advance Refractive Prediction System (AREPS v.3.03) software package.

References

1. INTRODUCTION

Since the tropospheric refractive index is frequency independent, the lower parts of the atmosphere affect the radiowave propagation in a wide frequency range, from VHF to optical frequencies, whereas, abnormal environmental conditions can end up to ducting phenomena. These result to the trapping of the UHF radio waves and contribute to the over-the-horizon propagation. The modeling of radio wave propagation through the troposphere has been extensively studied, and nowadays a great number of reliable models are in use.

In the past, emphasis was given to geometrical optics techniques. These methods [1—3] provide a general geometrical description of ray families, propagating through the troposphere. They are based on the discrimination of the medium into sufficiently small segments, with a linearly varying modified refractivity index. In each segment, the radiowave propagating angle is calculated using either the Snell's law or its generalized form, if the Earth's curvature is considered. These methods have main advantages, since their implementation is very simple and the necessary CPU time is very small. On the other hand, ray tracing methods present many disadvantages; for example the radiowave frequency is not accounted for and it is not always clear whether the ray is trapped by the specific duct structure [4].

An alternative approach for tropospheric propagation modeling was developed by Baumgartner [5] and was extended and improved by Baumgartner [6] and Shellman [7]. This method, usually known as Waveguide Model or Coupled Mode Technique, is based on a root finding algorithm by tracing the curve defined by

$$G = |R(\theta)R_g(\theta)| = 1 \tag{1}$$

where

R	is a complex reflection coefficient over the height h_0,
R_g	is the corresponding coefficient below the height h_0,
h_0	is a reference height.

This is used to determine the eigenangles θ_n, that have a practical meaning in tropospheric propagation. These are inserted in a height-gain differential equation calculating the propagation factor. The main disadvantages of coupled mode techniques lie in the complexity of the root finding algorithms and the large computational demands,

especially when higher frequencies and complicated ducting profiles are involved.

One of the most reliable and widely used techniques is the Parabolic Equation (PE) Method, initially developed for the study of underwater acoustics problems and later on extended to tropospheric propagation ones. The PE is based on the solution of the two-dimensional differential parabolic equation, fitted by homogeneous or inhomogeneous refractivity profiles. The calculations take into account the radius of the Earth and terrain effects whereas the polarization of the propagating radiowaves is implemented on the surface boundary conditions. The direct global solution of the PE, by means of a numerical method e.g., Finite-Difference Time-Domain (FDTD) or FEM, results to a complex system of equations, the solution of which requires high computational power and large RAM.

In this work, the parabolic equation is properly manipulated to a one-dimensional form, the solution of which is achieved using the Finite Element Method (FEM). The solution advances in space using small range steps. The total field is determined in a two-dimensional tropospheric medium, since azimuth symmetry is assumed. Finally, radar application examples are presented, demonstrating the radio wave propagation under surface ducting conditions, while the method is evaluated through a comparison to the corresponding results from the AREPS package, under the same propagation conditions.

2. TROPOSPHERIC DUCTS

The index of refraction is defined as

$$n = \sqrt{\varepsilon_r} = c/v \tag{2}$$

where

ε_r	is the dielectric constant of the troposphere,
c	is the speed of light and
v	is the phase velocity of the electromagnetic wave in the medium.

Since n near the earth's surface is slightly greater than unity (1.00025–1.00040), it seems more practical to use the scaled index of refraction N, which is called refractivity and is defined as [8]:

$$N = (n-1) \cdot 10^6 = \frac{77.6p}{T} - \frac{5.6e}{T} + \frac{3.75 \cdot 10^5 e}{T^2} \tag{3}$$

where

p is the total pressure in mbar,
e is the water vapor pressure and
T is the temperature in °Kelvin.

In order to examine the N gradients, the modified refractivity index is used. It is defined as [9]:

$$M = \left(n - 1 + \frac{h}{a}\right) \cdot 10^6 = N + 0.157h \tag{4}$$

The computation of the refractive conditions, characterized as Subrefraction, Standard, Surerrefraction and Trapping is achieved by its gradient dM/dh. Tropospheric ducting phenomena occur when either:

$$\frac{dM}{dh} < 0 \tag{5a}$$

or

$$dN/dh < -157 \tag{5b}$$

is met.

The tropospheric ducting effects to radio wave propagation, are similar to that of the metal waveguides; therefore, only modes with a wavelength shorter than the cut-off wavelength can propagate (the cut-off frequency being a function of the duct's width). In transmitter/receiver systems, the height of the antennas, together with the vertical refractivity profile, can lead to a variety of phenomena. Usually, the radio waves are trapped inside the duct, leading to an over-the-horizon propagation. On the other hand, a radar with the antenna positioned below the ducting layer can miss a target flying inside or above the duct. If both receiving and transmitting antennas are located inside the duct, the field in the receiver is stronger, compared to the field received in the absence of the waveguide.

3. PARABOLIC EQUATION

Various methods for the solution of the PE were developed and presented to the day. The most efficient algorithm seems to be the Split Step Solution which employs the Fast Fourier Transform (FFT) to advance the solution over small range steps. The algorithm has been widely used in many applications [10, 11, 4]. More specifically, Barrios [12, 13] treated horizontally inhomogeneous environments and a terrain model respectively. Craig and Levy [14] applied the Split

Step Solution to assess radar performance under multipath and ducting conditions. Finally, Sevgi and Paker [15] discussed the path loss in HF propagation channels. Alternative algorithms for the solution of the PE were also proposed. For example, Levy [16] presented a Finite-Difference formulation, whereas she has also applied [17], the horizontal PE solution above a specific height level. Finally, Akleman and Sevgi [18], applied a Finite-Difference Time-Domain (FDTD), and extended its algorithm [19] in order to deal with varying terrain models.

The analysis to follow starts from a Parabolic Equation form taking into account the Earth flattening transformations [4, 20]:

$$\frac{\partial^2 u(x,z)}{\partial z^2} + 2jk\frac{\partial u(x,z)}{\partial x} + k^2\left(n^2 - 1 + \frac{2z}{R}\right)u(x,z) = 0 \qquad (6)$$

Where $k = 2\pi/\lambda$ is the free space wave-number,

x is the horizontal propagation distance (range),
z is the heightand
R is the Earth′s radius (6378165 m).

Assuming that the field slowly varies in the x direction, the partial derivative $\partial u(x,z)/\partial x$, can be analyzed to its partial variations. Thus, for a sufficiently small range step δx, Equation (6) can be written as:

$$\frac{\partial^2 u(x,z)}{\partial z^2} + 2jk\frac{u(x,z) - u(x-\delta x,z)}{\delta x} + k^2\left(n^2 - 1 + \frac{2z}{R}\right)u(x,z) = 0 \qquad (7)$$

or

$$\frac{\partial^2 u(x,z)}{\partial z^2} + \left[\frac{2jk}{\delta x} + k^2\left(n^2 - 1 + \frac{2z}{R}\right)\right]u(x,z) = \frac{2jk}{\delta x}u(x-\delta x,z) \qquad (8)$$

Assuming $x = \delta x$, the quantity $u(x-\delta x,z) = u(0,z)$ corresponds to the initial field. Equation (8) is a recursive, one-dimensional form of the parabolic equation. For each range step , it can be directly solved using FEM and the resulting solution is introduced as an excitation to the equation of the next step. The refractive index, n, is directly assigned to each line element of the FEM mesh and thus, any complex or fast varying medium profile can be modeled.

It is obvious that for the first range step, the initial field $u(0,z)$ is required. It can be any function of z, numerical or analytical, depending on the specific problem demands. Thus, the starting field can simulate the far field of any antenna. In the applications presented

here, a Gaussian shaped field is used, representing the main lobe of a radar system and it is expressed by the Gaussian relation [21]:

$$W(z) = A \exp\left(-\frac{(z - H_0)^2}{k_f}\right) \tag{9}$$

Where

$W(z)$	is the magnitude of the field in respect to height,
H_0	is the altitude of the radar antenna,
A	is the maximum intensity of W at height H_0 and
k_f	is a coefficient which determines the beam width.

4. BOUNDARY CONDITIONS

The solution of equation (8) using FEM, requires the application of boundary conditions at the starting height, $z = z_{\min}$, which in fact is the Earth's surface, and at the maximum altitude considered, $z = z_{\max}$. At the upper artificial boundary, an absorbing condition has to be applied, allowing for the propagation of the waves and at the same time, reducing any possible reflections introduced by the method. Therefore, a first or second order absorbing boundary condition is applied [22], combined with the $z_{\max}$ extension. Alternatively, the non-desirable upper boundary reflections can be eliminated by applying a fictitious absorber or a Perfectly Matched Layers (PML) scheme.

The entrance boundary conditions are expressed by the equation:

$$\left[\frac{\partial u}{\partial z} + jkqu\right]_{z=z_{\max}} = 0 \tag{10}$$

Where q is given by:

$$q = q_v = \sqrt{\frac{\mu_r}{\left(\varepsilon_r + \dfrac{j\sigma}{\omega\varepsilon_0}\right)}} \tag{11}$$

or:

$$q = q_H = \sqrt{\frac{\left(\varepsilon_r + \dfrac{j\sigma}{\omega\varepsilon_0}\right)}{\mu_0}} \tag{12}$$

for vertical and horizontal polarization respectively. In the equations (11) and (12), ε_r, μ_r are the relative permittivity and permeability

of the medium (surface) respectively, ε_0, μ_0, the permittivity and permeability of the free space, and σ is the absolute ground conductivity. For a perfectly conducting surface, equations (11) and (12) are reduced to $\partial u(x,0)/\partial z = 0$ for vertical polarization and $u(x,0) = 0$ for horizontal polarization, whereas for an imperfectly conducting ground surface, the above equations can be applied using for example [17] $\varepsilon_r = 15$ and $\sigma = 0.01\,\mathrm{S/m}$.

5. WAVE SEPARATION

The solution of equation (8) using the marching algorithm discussed in the previous sections, gives the total field u, which is the combination of the upwards and downwards propagating coefficients. The wave separation methodology, initially introduced for the discrimination of radio waves after their reflection from the ionosphere [23] is based in the application of the Discrete Fourier Transform (DFT) in the space domain. In figure 1a, the coverage contour plot, representing the total field of a wide vertically polarized radar beam ($K_f = 11000$) under a surface duct, is shown. The carrier frequency is 1 GHz and the ground surface is taken as perfectly conducting. The upper artificial boundary condition was set to be non-perfectly absorbing. Thus, the reflections occurring at 300 m are due to the surface duct, while the reflections arising at the upper boundary located at 1000 m, are due to the upper boundary conditions.

Since the global solution is calculated using a marching range scheme, the Fourier components amplitude versus the normalized space-frequency (m^{-1}) is plotted, applying the DFT at the height solution of each range step (Fig. 1(b)). In this figure, the lower components represent the up-going traveling waves, while the higher components represent the descending waves. Isolating these components and applying the Inverse DFT, the up and down going waves are separated (Figs. 1(c) and 1(d)). Of course, the algebraic summation of these components will give the initial total field. The above example corresponds to one of the worst cases, where both the artificial boundary and the tropospheric duct reflect a portion of the incident waves and it is used to demonstrate the separation method. It is obvious that using a perfectly absorbing boundary condition or a PML scheme, the reflections from the atmospheric ducts are clearly determined. On the other hand, if standard atmospheric conditions are assumed, any possible reflections are due to the upper artificial boundary only, allowing for the evaluation and the design of improved absorbing layers or conditions.

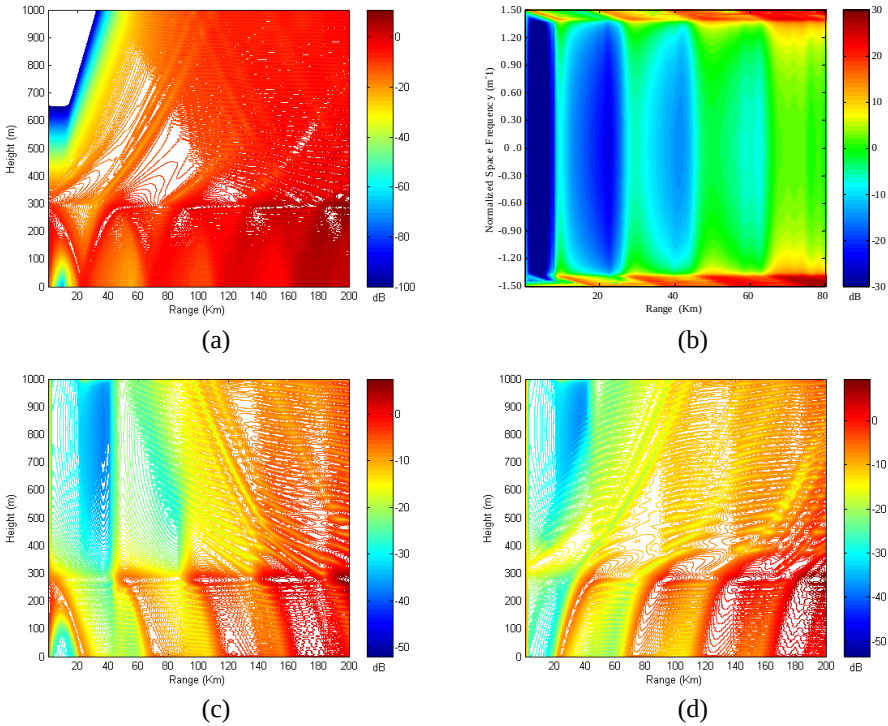

Figure 1. Wave separation example.

6. RESULTS AND DISCUSSION

In order to demonstrate the results obtained using the FEM solution of the PE, the method was applied to various frequencies and medium profiles. A radar antenna located at a height of 150 m above the see level was assumed in all the examples of this section,. The main lobe beam was modeled according to equation (9), with $H_0 = 150$ and $A = 1$. Moreover, vertical polarization and a perfectly conducting ground were assumed. The solution of the final system of the FEM equations was obtained using the Bi-Conjugate Gradients stabilized method for a faster convergence. Other solution methods can be implemented as well, as for example the Bi-Conjugate Gradients and the Conjugate Gradient Squared methods.

Figure 2 presents the coverage diagram of a narrow radar beam ($K_f = 11$) at 100 MHz, under various tropospheric conditions for standard atmospheric conditions [9]. It can be seen that the

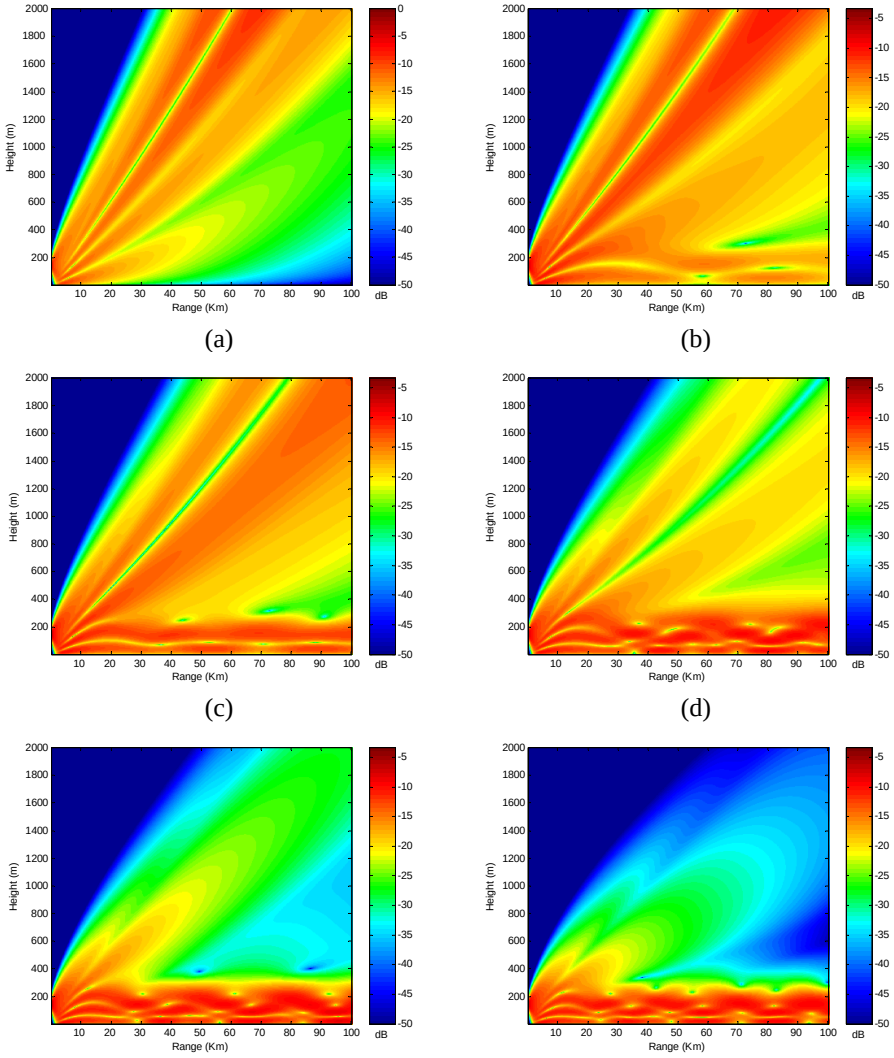

Figure 2. Propagation at 100 MHz under various tropospheric profiles.

waves propagate undisturbed through the tropospheric medium. In Figures 2(b) to 2(f), a bilinear surface ducting profile was included, starting from the sea level to an altitude of 300 m. Standard atmospheric conditions over this altitude were also assumed, while the waveguide intensity was set to increase by steps of −0.5 M-units/m in each diagram. This example illustrates the trapping mechanism and it is clear that as the ducting intensity increases, a greater amount of the propagating energy is restricted inside the waveguide region. Especially, in the extraordinary atmospheric profiles assumed in Figures 2(e) and 2(f), the waves are almost completely trapped between the see level and 300 m.

Figure 3 demonstrates a more realistic tropospheric propagation example through a ducting medium profile, incorporating frequency bands mainly used by terrestrial search radar systems. The waveguide intensity was set to −1 M-units/m for the first 300 m, and standard atmosphere above this altitude. Figures 3(a) and 3(b) show the

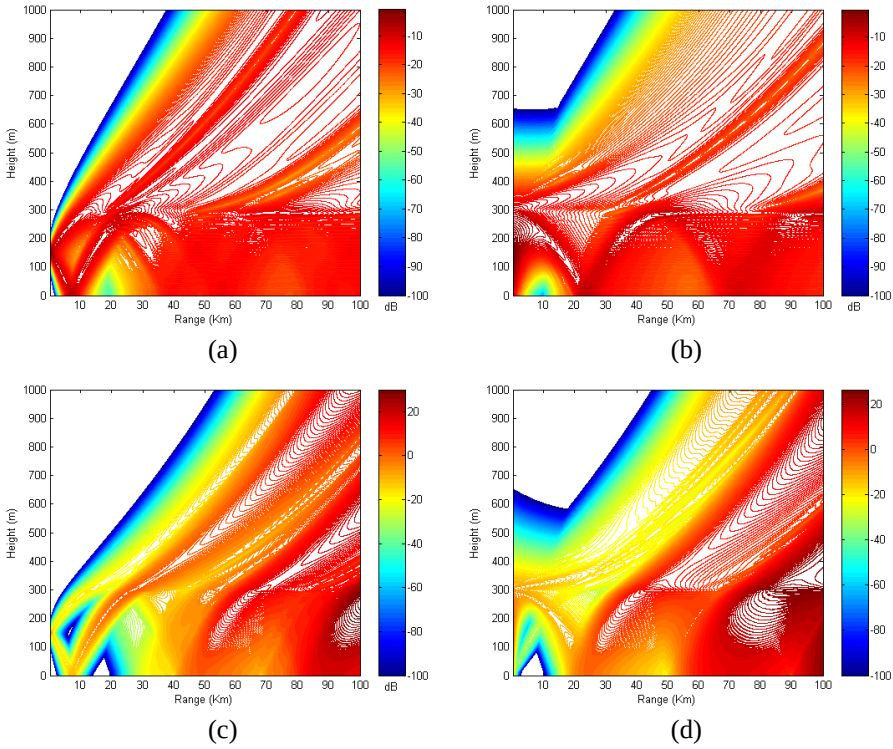

Figure 3. Narrow and wide beam propagation at 1 and 3 GHz.

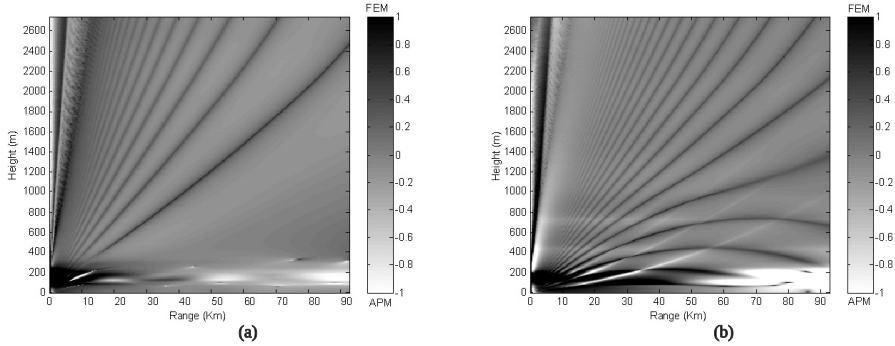

Figure 4. FEM and APM methods normalized differences (dB) at 100 and 200 MHz.

coverage contour diagrams (0.5 dB levels), for a carrier frequency at 1 GHz. In these figures, the vertically polarized beam width factor is taken to be $k_f = 11$ (narrow beam) and $kf = 11000$ (wide beam) respectively. Figures 3(c) and 3(d) demonstrate the propagation at 3 GHz, for the conditions applied in Figures 3(a) and 3(b). In these figures, the trapping of the waves below 300 m is obvious, especially at the frequency of 1 GHz. Moreover, the troposphere shows a leaky waveguide behavior since it does not trap the whole amount of the propagating energy.

Even if the refractive index of the troposphere is frequency independent, it can be seen that the coverage diagrams vary between the 1 and 3 GHz, since the frequency is included in the main parabolic equation (6) and (8), via the wave number $k = 2\pi/\lambda$. This is an advantage in respect to ray tracing techniques, where both frequencies would result in the same coverage diagrams. It can also be seen (Figures 3(b) and 3(d)) that since the wide beam radar antenna is located inside the ducting region, the transmitted wave is divided into two components; an up-going, which overcomes the trapping condition and a descending, which undergoes ground reflections.

In order to validate the FEM solution of the PE, the results were compared to those obtained by the AREPS. The AREPS program computes and displays a number of tactical decision aids to assess the influence of the atmosphere and terrain on the performaces of electromagnetic (EM) systems. The internal propagation model used by AREPS is the Advance Propagation Model (APM). This is a hybrid model that consists of four sub-models: flat earth, ray optics, extended optics, and split-step parabolic eqation (PE). APM effectively merges the Radio Physical Optics (RPO) model [24, 25, 26] with the Terrain

Parabolic Equation Model (TPEM) [13].

In figures 4(a) and 4(b), the normalized propagation factor differences between the results obtained using the FEM and the APM methods, are shown. The examples illustrate the propagation of a horizontally polarized Gaussian beam (Beam Width = 4°) at 100 and 200 MHz respectively. In figure 4(a), a surface duct is assumed (dM = -1 M-units/m), having its top at 300 m above an imperfectly conducting ground surface ($\varepsilon_r = 15, \sigma = 0.01$ S/m) and above this altitude standard atmospheric conditions were applied. Similarly, in figure 4(b) the propagation characteristics are the same, while the duct's top was extended to 1000 m above the surface and its strength is lowered to 0.3 M-units/m. It can be seen that the differences between the two methods are very small and in general they do not exceed 1 dB. Moreover, the maximum deviations are located around the initial field region and they are probably caused by small differences in the way that the source antenna far-field is applied in FEM and APM methods.

7. CONCLUSIONS

In practice, the FEM formulation can easily process complex refractivity profiles of any kind, either numerical or analytical. Moreover, the refractive index being independent between consequent range steps, gives the ability to include horizontally inhomogeneous tropospheric profiles. In these cases, the method's response can be directly adjusted to the refractivity variations, by properly modifying the size of the FEM elements and the range step.

The proposed technique for the separation of the incident and reflected wave components provides a useful tool for many applications. For example, this methodology can be used for the determination of the reflection coefficients and their space distribution. Moreover, it can be used for the of the upper absorbing boundary conditions efficiency evaluation, since the unwanted scattered field components can be calculated.

REFERENCES

1. Hitney, H. V., "Refractive effects from VHF to EHF. Part A: Propagation mechanisms," AGARD-LS-196, 4A-1–4A-13, 1994.
2. Patterson, W. L., C. P. Hattan, G. E. Lindem, R. A. Paulus, H. V. Hitney, K. D. Anderson, and A. E. Barrios, "Engineer's refractive effects prediction systems (EREPS) version 3.0," NRaD Technical Document 2648, May 1994.

3. Lear, M. W., "Computing atmospheric scale height for refraction corrections," NASA Mission Planning and Analysis Division, Lyndon B. Johnson Space Center, 1980.
4. Slingsby, P. L., "Modeling tropospheric ducting effects on VHF/UHF propagation," *IEEE Transactions on Broadcasting*, Vol. 37, Issue 2, 25–34, 1991.
5. Baumgartner, G. B., H. V. Hitney, and R. A. Pappert, "Duct propagation modeling for the integrated-refractive-effects prediction program (IREPS)," *IEE Proc., Pt. F*, Vol. 130, No. 7, 630–642, 1983.
6. Baumgartner, G. B., "XWVG: A waveguide program for trilinear tropospheric ducts," Tech. Doc. 610, Naval Ocean Systems Center, ADA133667, 1983.
7. Shellman, C. H., "A new version of MODESRCH using interpolated values of the magnetoionic reflection coefficients," Interim technical report NOSC/TR-1143, Naval Ocean Systems Center, ADA179094, 1986.
8. Flock, W. L., "Propagation effects on satellite systems at frequencies below 10 GHz," *A Handbook for Satellite System Design*, Second edition, NASA Reference Publication 1108 (02), 1987.
9. ITU-R, "The radio refractive index: its formula and refractivity data," International Telecommunication Union, Recommendation 453–459, 2003.
10. Craig, K. H., "Propagation modeling in the troposphere: Parabolic equation method," *IEEE Electronics Letters*, Vol. 24, Issue 18, 1136–1139, 1988.
11. Dockery, G. D., "Modeling electromagnetic wave propagation in the troposphere using the parabolic equation," *IEEE Transactions on Antennas and Propagation*, Vol. 36, Issue 10, 1464–1470, 1988.
12. Barrios, A. E., "Parabolic equation modeling in horizontally inhomogeneous environments," *IEEE Transactions on Antennas and Propagation*, Vol. 40, Issue 7, 791–797, 1992.
13. Barrios, A. E., "A terrain parabolic equation model for propagation in the troposphere," *IEEE Transactions on Antennas and Propagation*, Vol. 42, Issue 1, 90–98, 1994.
14. Craig, K. H. and M. F. Levy, "Parabolic equation modelling of the effects of multipath and ducting on radar systems," *IEEE Proc. F*, Vol. 138, No. 2, 153–162, 1991.
15. Sevgi, L. and S. Paker, "Surface wave path loss calculations in HF propagation with split-step parabolic equation," *Proc.*

of PIERS'96, Progress In Electromagnetic Research Symposium, Vol. 1, 67, Innsbruck, Austria, July 8–12, 1996.

16. Levy, M. F., "Parabolic equation modeling of propagation over irregular terrain," *IEEE Electronics Letters*, Vol. 26, No. 14, 1153–1155, 1990.
17. Levy, M. F., "Horizontal parabolic equation solution of radiowave propagation problems on large domains," *IEEE Transactions on Antennas and Propagation*, Vol. 43, Issue 2, 137–144, 1995.
18. Akleman, F. and L. Sevgi, "A novel finite-difference time-domain wave propagator," *IEEE Transactions on Antennas and Propagation*, Vol. 48, No. 3, 839–843, 2000.
19. Akleman, F. and L. Sevgi, "Realistic surface modeling for a finite-difference time-domain wave propagator," *IEEE Transactions on Antennas and Propagation*, Vol. 51, No. 7, 1675–1679, 2003.
20. Ko, H. W., J. W. Sari, M. E. Thomas, P. J. Herchenroeder, and P. J. Martone, "Anomalous propagation and radar coverage through inhomogeneous atmospheres," *AGARD Conf. Proc.*, Vol. 346, AGARD-CP-346, 1–14, 1984.
21. Salonen, K., "Observation operator for Doppler radar radial winds in HIRLAM 3D-Var," *Proceedings of ERAD (2002)*, 405–408, Copernicus GmbH, 2002.
22. Jin, J., *The Finite Element Method in Electromagnetics*, John Wiley & Sons, New York, 1993.
23. Isaakidis, S. A. and Th. D. Xenos, "Wave propagation and reflection in the ionosphere. An alternative approach for ray path calculations," *Progress In Electromagnetic Research*, PIER 45, 201–215, 2004.
24. Hitney, H. V., "Hybrid ray optics and parabolic equation methods for radar propagation modeling," *IEE International Conference 365, "Radar 92"*, 58–61, Oct. 1992.
25. Patterson, W. L. and H. V. Hitney, "Radio physical optics CSCI software documents," NCCOSC RDTE DIV Technical Document 2403, Dec. 1992.
26. Patterson, W. L. and H. V. Hitney, "Radio physical optics (RPO) CSCI software documents, RPO Version 1.16," NCCOSC RDTE DIV Technical Document 2403, Rev. 1, Apr. 1992.

Stergios A. Isaakidis received a Diploma in Electrical Engineering from the Engineering Department of the Hellenic Air Force Academy and he is a Ph.D. Candidate in Aristotle University of Thessaloniki. He

is Electronic Intelligence officer and Communications and Electronic Warfare engineer in the Hellenic Air Force.

Thomas D. Xenos received a Diploma in Electrical Engineering from the University of Patras and a Ph.D. in Radio Wave Propagation from the Aristotle University of Thessaloniki. He is Associate Professor of Electrical Engineering in the Aristotle University of Thessaloniki.